Sains Malaysiana 47(5)(2018): 1025–1031
http://dx.doi.org/10.17576/jsm-2018-4705-19

Preparation and Characterization of Macroporous Bioactive Glass Ceramic Made via Sol-Gel Route and Powder Sintering Method

(Penyediaan dan Pencirian Seramik Kaca Bioaktif Bermakroliang Dibuat Melalui Laluan Sol-Gel dan Kaedah Sinteran Serbuk)

SYED NUZUL FADZLI SYED ADAM*, ROSLINDA SHAMSUDIN, SITI ROHANI ZAINUDDIN, BANJURAIZAH JOHAR & FIRUZ ZAINUDDIN

ABSTRACT

The purpose of this study was to prepare macroporous glass ceramic scaffold by sol-gel glass synthesis and powder sintering method. Sodium nitrate was added during sol-gel process to obtain glass ceramic with mol composition of 42.11% SiO_2 - 18.42% CaO - 29.82% Na_2O - 9.65% P_2O_5. The glass particles were found to be thermally stable above 900°C as indicated by TGA/DTA analysis. The dried glass particles obtained from sol-gel process were compacted and sintered at 1000°C for 3 h soaking time. Sintering crystallized the glass by 71.5% of crystallinity with tetracalcium catena-hexaphosphate (V) ($Ca_4(P_6O_{19})$) as the main crystalline phase as revealed by XRD analysis. Although glass crystallized during sintering, it showed a good in vitro *bioactivity as apatite-like layer were deposited on the glass ceramic surface when immersed in simulated body fluid (SBF) for 14 days. SEM analysis proved the macroporous structure formation with pore size ranges between 30 and 350 µm due to foaming effect which occurred during sintering. Besides that, the glass ceramic surface formed into vitrified-like due to fluxing effect during sintering thus affected the porosity and densification measurement done by Archimedes test. In conclusion, the presence of sodium oxide in sol-gel glass ceramic composition by 29.82 mol % with sintering temperature at 1000°C is able to produce bioactive and macroporous glass ceramic that potentially be used as medical scaffold material.*

Keywords: Glass ceramic; macroporous; powder sintering; scaffold; sol-gel

ABSTRAK

Tujuan kajian ini dijalankan adalah untuk menyediakan perancah seramik kaca bermakroliang melalui kaedah sintesis sol-gel dan sinteran serbuk. Natrium nitrat telah ditambahkan semasa proses sol-gel untuk menghasilkan seramik kaca dengan komposisi mol iaitu 42.11% SiO_2 - 18.42% CaO - 29.82% Na_2O - 9.65% P_2O_5. Partikel kaca didapati stabil secara terma pada suhu melebihi 900ºC seperti yang ditunjukkan oleh analisis TGA/DTA. Partikel kaca kering yang diperoleh daripada proses sol-gel dipadatkan dan disinter pada suhu 1000ºC selama 3 jam. Sinteran menghablurkan kaca sebanyak 71.5% kehabluran dengan tetrakalsium katena-heksafosfat (V) ($Ca_4(P_6O_{19})$) sebagai fasa berhablur utama seperti yang ditunjukkan oleh analisis XRD. Walaupun kaca menghablur semasa sinteran, sampel masih menunjukkan kebioaktifan in vitro *yang baik disebabkan lapisan seakan apatit termendap di atas permukaan seramik kaca selepas direndam dalam larutan bendalir badan simulasi (SBF) selama 14 hari. Analisis SEM membuktikan pembentukan struktur bermakroliang dengan julat saiz liang antara 30 ke 350 µm disebabkan oleh kesan pembusaan yang berlaku semasa sinteran. Selain itu, permukaan seramik kaca membentuk seakan kekaca disebabkan oleh kesan fluks semasa sinteran sekaligus menjejaskan pengukuran keliangan dan pemadatan melalui ujian Archimedes. Kesimpulannya, kehadiran komponen natrium oksida dalam komposisi seramik kaca sol-gel sebanyak 29.82% mol dengan suhu sinteran pada 1000°C dapat menghasilkan seramik kaca bioaktif dan bermakroliang yang berpotensi untuk digunakan sebagai bahan perancah perubatan.*

Kata kunci: Bermakroliang; perancah; seramik kaca; sinteran serbuk; sol-gel

INTRODUCTION

Biomaterial must meet several requirements in order to be used as bone scaffold and one of them is possess macroporous structure with pore size ranges from 100 to 500 µm (Chen & Boccaccini 2006; Guarino et al. 2007; Rezwan et al. 2006). Scaffolds with pore size at 100 µm favor the formation of tissue ingrowth while pore size exceed 300 µm encourage ingrowth of bone besides the formation of capillary (Karageorgiou & Kaplan 2005; Liu et al. 2013a). Numerous studies have been conducted in preparing macroporous ceramic scaffold which involved techniques such as polymer burnout, foam synthesis and template replication method (Chen & Boccaccini 2006; Jones et al. 2006; Liu et al. 2013a; Stábile et al. 2015; Wu et al. 2011). These techniques particularly produced highly interconnected porous structures, however lack in mechanical strength (Izadi et al. 2014; Jones et al. 2006; Liu et al. 2013b).

Certain composition of glass is known to have the ability to bond directly with bone without having fibrillary connective tissue between materials and bone. This type of material known as bioactive glasses exhibited non-toxic properties, biocompatible and match the natural bone composition (Mehdikhani & Borhani 2013). The bioactive behavior is proved by the formation of apatite layer and it is important for bonding with living bone (Duée et al. 2007). Various benefits provided by bioactive glass indicate its high potential as scaffolds materials in orthopedic applications. However, glass utilizations as scaffold material is limited due to its brittleness and lack in mechanical properties. Sintering is known to cause crystallization of glass and turn this amorphous material into glass ceramic phase which may enhanced their mechanical properties due to densification, formation of crystallized phases and grain growth (Siqueira et al. 2011; Stábile et al. 2015).

We have found that, there were very limited studies on sintering of glass particles in preparation of macroporous scaffolds due to the fact that sintering is known to reduce the glass initial bioactivity (Izadi et al. 2014; Liu et al. 2013b; Sabree et al. 2015). However, recent study also showed the sintered glass especially the one that contained high percentage of network modifier such as calcium and sodium has maintained or even increased their bioactivity property (Esfehani et al. 2013; Jones et al. 2010; Kamalian et al. 2012). Because of that, a promising method which optimized sintering parameters in producing glass ceramic scaffold with sufficient mechanical strength while preserving its bioactive property is needed.

Sol-gel derived glasses were typically known to have nanoporous structure caused by the gelation and drying process involved in the sol-gel process (Jones 2009; Saravanapavan & Hench 2003). However, these nanopores are particularly not sufficient as scaffold materials since macro-size pores are required. Our early observation has found that, addition of sodium nitrate into sol-gel glass composition then followed by powder sintering is able to produce macroporous glass ceramic structure with promising mechanical strength. Hence, further studies needs to be carried out regarding this subject. Thus, the aim of this study was to prepare macroporous glass ceramic by sol-gel route and powder sintering method and characterized its properties including the glass initial powder characteristic, surface morphology, phases and *in vitro* bioactivity of the sintered bodies.

Materials and Methods

Glass particles with composition of 42.11% SiO_2 – 18.42% CaO – 29.82% Na_2O – 9.65% P_2O_5 (based on mol %) was prepared via acid catalyzed sol-gel method at ambient temperature. Forty mL of deionized water was mixed with 1 mL of nitric acid (1 M) and the solutions were stirred on a magnetic stirrer. Reagents and precursors were added during this process by following the sequence of 10 mL of tetraethyl orthosilicate (TEOS), 2 mL of tetraethyl phosphate (TEP) and 5 g of calcium nitrate tetrahydrate by allowing the solution under continuous stirring for half an hour for each reagent added. Then, 3.0 g of sodium nitrate were added into the solution and stirring was continued for another 1 h. The sol obtained then casted into the polyethylene mold and left at ambient temperature for overnight until gelation occurred. The wet gel was dried at 120°C before thermally stabilized at 600°C. Dried gel was ground using agate and mortar to obtain fine particles.

The glass particles characteristics were analyzed using Malvern particle sizer, Thermal Gravimetric Analysis (TGA)/Differential thermal analysis (DTA) and Scanning Electron Microscope (SEM). The glass particles were pressed into cylindrical pellets via uniaxial powder press before sintered at 1000°C for 3 h. The sintered pellets were also analyzed with Archimedes test, Scanning Electron Microscopy (SEM) with Energy Dispersive Spectroscopy (EDS) and X-ray Diffraction (XRD). The *in vitro* bioactivity test of sintered glass was conducted by immersion into simulated body fluid (SBF) for 14 days. The immersed samples were rinsed with acetone and dried in desiccator. The apatite-like phase deposited on the sample surface was observed by mean of Scanning Electron Microscopy (SEM) and EDX.

Result and Discussion

Particle Size Analysis (PSA)

Figure 1 shows the particle size distribution of sol-gel derived glass powder after thermal stabilized at 600°C. The glass showed a wide particle sizes distribution ranging from 0.550 μm to 724.436 μm as this powder did not undergo intensive milling and sieving process. The huge range size obtained may also indicate the agglomeration of the particles. However, the glass particle sizes are in monomodal distribution. According to Wachi and Jones (1992), monomodal distribution indicates no significant agglomerations occurred among the glass powder after thermal stabilization. The glass particles size was also proved to be inhomogeneous (huge differences in size) and no apparent agglomeration of particles was observed by SEM image in Figure 2. The highest volume particle size distribution of the glass powder is showed approximately at 138.038 μm and smaller fraction of the glass particles also has achieved in nanometer size range.

Thermal Analysis

Figure 3(a) and 3(b) shows the TGA and DTA analysis for sol-gel glass powder after thermal stabilized at 600°C, respectively. There were four stages of weight losses were observed where the first stage occurred at temperature range between 40°C to 100°C due to the removal of absorbed water and pore liquor as associated to the endothermic peak in DTA at 60°C (Bizari et al. 2013; Jones et al. 2006; Mozafari et al. 2010; Mukundan et al. 2013; Saboori et al.

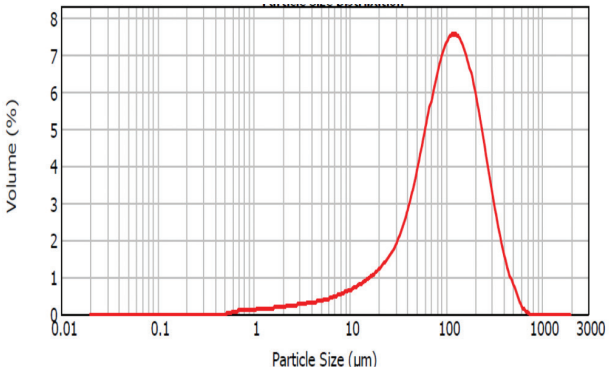

FIGURE 1. Particle size distribution of gel glass powder thermal stabilized at 600°C

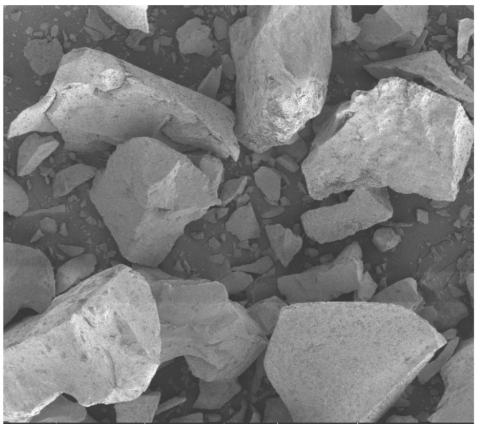

FIGURE 2. SEM image of gel glass particle after thermal stabilized at 600°C

2009; Saravanapavan et al. 2003). The second mass loss has occurred at temperature between 100°C to 600°C in which exothermic peak at 260°C indicated that chemically absorbed water was released (Mukundan et al. 2013). It was noticed that a small exothermic peak at 300°C was presence due to the loss of the organic compound such as those in alkoxysilane group.

The third mass loss occurred onset around 600°C until 900°C. Within these range, typically nitrates and carbonates residual were eliminates (Bizari et al. 2013; Delben et al. 2013; Izquierdo et al. 1999; Mozafari et al. 2010). The fourth mass loss occurred onwards temperature of 900°C which commonly associated with crystalized phase formation. The exothermic peak approximately at 970°C occurred due to the crystallization of phase such as $CaSiO_3$ (β-wollastonite) (Izquierdo et al. 1999). The crystalline wollastonite phase is able to improve the hardness of the glass ceramic (Liu & Miao 2004). This result also suggested that at temperature above 970°C, glass-ceramic can be obtained and the sample also effectively gain stability at temperature around 900°C. This glass ceramic phase has started to melt at temperature above 1000°C before being fully melted approximately at 1260°C. Thus, from this TGA analysis, the glass sintering temperature used in this study is set at 1000°C which is just below its melting point.

PHYSICAL AND MORPHOLOGICAL ANALYSIS

Figure 4 shows the glass ceramic morphology viewed from (a) surface, (b) horizontal cross section and (c) vertical cross section; meanwhile (d) surface elemental composition obtained via EDX analysis spot at point X. From EDX, the highest elements that present were Si-O and followed by Ca, Na and P. This elements were belongs to this glass ceramic composition, which is based on SiO_2-CaO-Na_2O-P_2O_5 system. The presence of C element is commonly observed for sol-gel sintered glass. The SEM images showed the significant formation of macropore structures observed on the entire glass ceramic surface. In average, the macropores were approximately achieved at 350 µm in size. The macropores can also be observed on the cross sectional surface of the glass ceramic in which

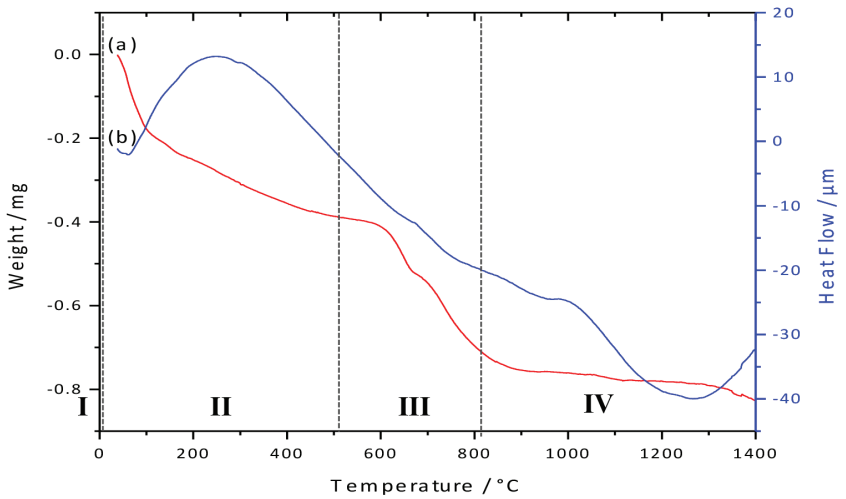

FIGURE 3. Graph of (a) thermal gravimetric analysis (TGA) and (b) differential thermal analysis (DTA) for gel glass powder thermal stabilized at 600°C

indicates continuous and connected open pores structures were obtained. This result indicates the potential of this technique in producing macroporous glass ceramic structure for scaffold implant material.

Table 1 shows the percentage of shrinkage, densification and apparent porosity of the glass ceramic obtained via Archimedes test. The samples expanded in thickness at 60.53% and shrunk at 4.35% in their diameter. The expansion in thickness was occurred due to foaming effect resulted from the released of gaseous during sintering. However, the apparent porosity measured is at only 6.83% by Archimedes test, thus caused high densification value was obtained for the glass ceramic which is at 93.17%. This is significantly contradicts with the apparent macroporous structures showed by previous morphological analysis (Figure 4). This is due to the fact that the sample surface was covered with flux after sintering thus forming a vitrified-like body, as glassy, smooth and hard sample surfaces were obtained.

This can be expected as sodium component is widely used in ceramic field as fluxing agent (Araújo et al. 2016; Brink et al. 1997; Nandi et al. 2011). This vitrified-like body lost of its nanopores structure and significantly resists the water absorption thru the surface and porosities. This leads to the low percentage of porosity and high percentage of densification obtained for the macroporous glass ceramic. This also indicates the Archimedes test is not an appropriate method in determines the porosity and densification for this glass ceramic scaffold. It is suggested to use an alternative tool such as XRD to determine this glass ceramic porosity and densification.

X-RAY DIFFRACTION ANALYSIS

Figure 5 shows the XRD diffractograms of the macroporous glass ceramic. Sintering at 1000°C cause crystallization and form glass ceramic phase as maximum diffraction peaks intensity was observed. Un-sintered sol-gel derived glass showed typical amorphous pattern (result not shown here). Sintering crystallized the glass by 71.5% of crystallinity with Tetracalcium Catena-Hexaphosphate (V) ($Ca_4(P_6O_{19})$ as the main crystalline phase with 39.2%. This is followed by Sodium Calcium Cyclo-hexasilicate ($Na_{5.27}Ca_3(Si_6O_{18})$), Disodium Dicalcium Disilicate ($Na_2Ca_2(Si_2O_7)$), Sodium Peroxide (Na_2O) and Silicon oxide (SiO_2) phases with 27.4%, 16.7%, 11.1% and 5.6%, respectively, as minor phases in the glass matrix. It should be noted that all elements (Si, O, Ca, P Na) existed in sample composition can be detected by XRD, suggesting that all elements are already existed as crystalline phase after sintering. The

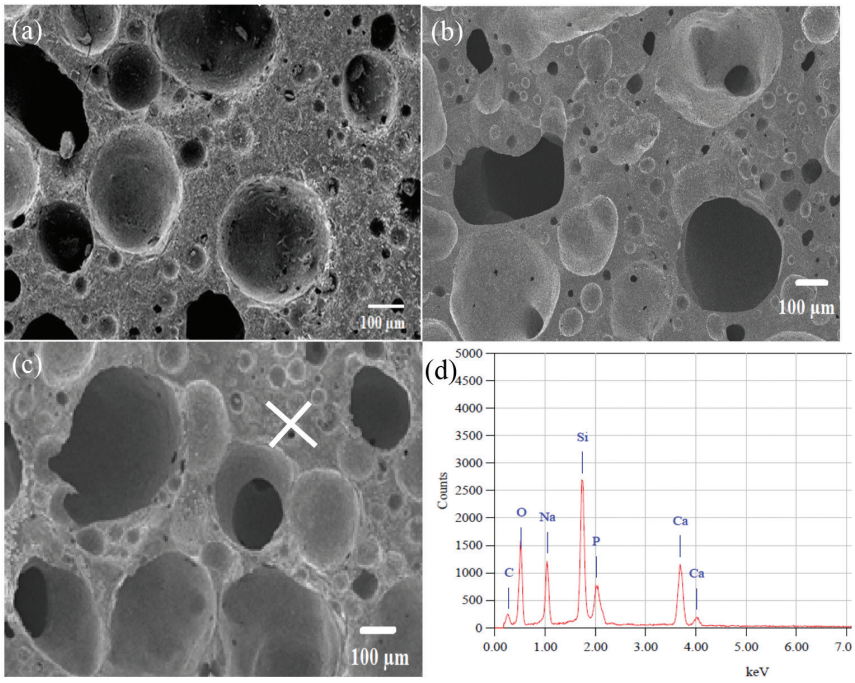

FIGURE 4. SEM image of (a) surface (b) horizontal cross section and (c) vertical cross section; meanwhile (d) is EDX graph of glass ceramic spot at X

TABLE 1. Percentage of shrinkage, densification and apparent porosity for glass ceramic

Sample property	Thickness expansion	Diameter shrinkage	Apparent porosity	Densification
Percentage (%)	60.53	4.35	6.83	93.17

presence of these phases also proved the formation of glass ceramic based on the quaternary system SiO_2-CaO-Na_2O-P_2O_5. Addition of sodium nitrate into the sol-gel glass composition significantly formed calcium phosphate and sodium oxide-related phases. This is similar with other findings (Mami et al. 2008) and also supported by previous TGA/DTA analysis (Figure 3) which shows exothermic reactions at temperature around 900°C due to the formation of calcium silicate and calcium phosphate related phases.

According to Shu et al. (2010), Tetracalcium Catena-Hexaphosphate ($Ca_4P_6O_{19}$) phase has a good chemical stability in SBF solution and only a small quantity of apatite-like particles can be formed on the scaffold surface after soaking in SBF solution for 28 days. However, they concluded that glass ceramics containing $Ca_4P_6O_{19}$ as main crystalline phase is bioactive and biocompatible even if no continuous apatite layer can be formed on scaffold surfaces after soaking in SBF for a period of time. According to several studies, the presence of sodium related phases will increased the glass ceramic mechanical properties and also possess degradable crystalline phases (Chen et al. 2010). Crystallization enhanced mechanical strength of the similar glass composition due to the formation of grains and grains boundaries (Bellucci et al. 2010; Chen et al. 2006). Thus, this glass ceramic should have better mechanical strength compared to its amorphous glass. However, further studies need to be conducted regarding this matter especially when they are in the form of macroporous structure.

IN VITRO BIOACTIVITY EVALUATION

Figure 6 shows the glass ceramic's (a) surface morphology, (b) macropores and (c) CaP rich structure after immersion in SBF for 14 days. Meanwhile Figure 6(d) shows the EDX analysis of the sample surface after immersion in SBF for 14 days. From the EDX, it was found that the concentration of CaP elements on the sample surface were increased compared to CaP content of un-immersed sample (Figure 4 (d)) due to increase deposition and growth of CaP rich structure. This proved the formation of apatite-like phase with Ca/P ratio of 1.62 within 14 days of immersion in SBF on the sample surface. This CaP rich structure can be observed on the surface (Figure 6(a)) and within the pores of the glass ceramic (Figure 6(b)) which indicates bioactivity reactions has been occurred during immersion in SBF. These CaP rich structure were highly deposited on the macroporous sites hence makes the macroporous are almost to be unseen.

Despite shows high crystallinity and vitrified surface, this glass ceramic showed good bioactivity property and this would be contributed by the macroporous structure. The addition of sodium nitrate in this glass composition was also important in favor the apatite formation. The presence of sodium (Na^+) and calcium (Ca^{2+}) network modifier cations interrupt the bridging oxygen (BO) bond which causes the formation of non-bridging oxygen (NBO) bond that improved the dissolution and bioactivity of glass ceramic and fasten the apatite nucleation (Liu et al. 2013; Sabree et al. 2015). According to previous study, slightly increase of Ca and P ion concentration in SBF is mainly attributed to the dissolving of $Ca_4P_6O_{19}$ phase and residual glass matrix (Shu et al. 2010), in which can contribute to the glass ceramic bioactivity.

Figure 6(d) shows the EDX analysis of the sample surface after immersion in SBF for 14 days. It was found that the concentration of Ca and P elements on the sample surface was increased compared to Ca and P content of un-immersed sample (Figure 4(d)) due to deposition and growth of apatite-like structure. This proved the formation of apatite-like phase with Ca/P ratio closed to 1.62 within 14 days of immersion in SBF on the sample surface.

CONCLUSION

Macroporous glass ceramic based on SiO_2-CaO-Na_2O-P_2O_5 has been successfully prepared via sol-gel route and powder sintering method. The addition of sodium nitrate into the initial glass composition during sol-gel process then followed by powder sintering at 1000°C enables a foaming effect occurred hence macropores structure were obtained. Despite crystallization occurred due to sintering, the glass ceramic proved to be bioactive. This study indicates the potential of macroporous bioactive glass ceramic to be prepared via this method. This macroporous bioactive glass ceramic is potentially be used as scaffold material in biomedical application.

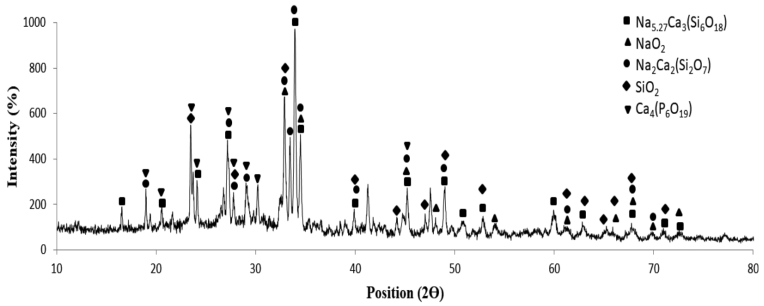

FIGURE 5. XRD analysis of glass ceramic sintered at 1000°C

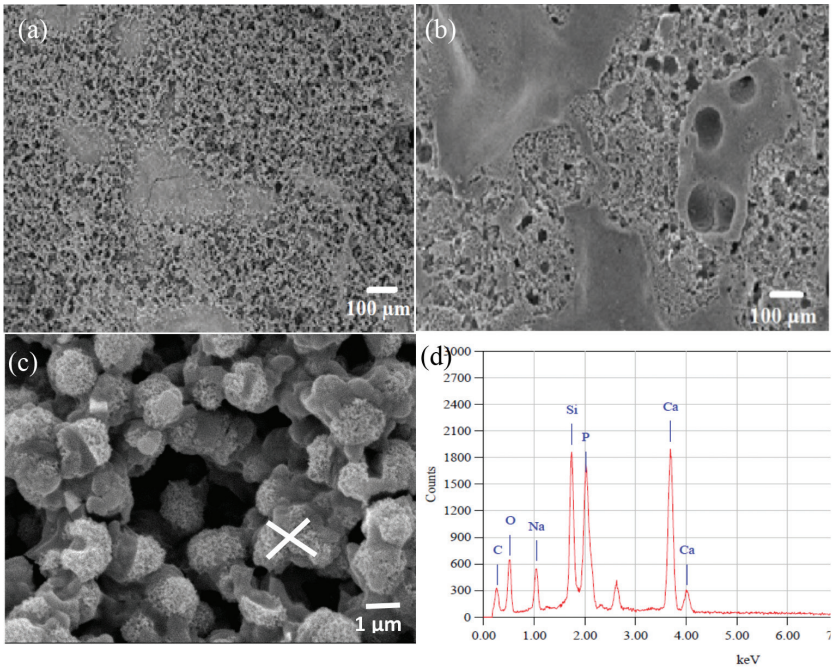

FIGURE 6. Formation of apatite-like layer on the glass ceramic (a) surface and (b) inside macropore structure. Meanwhile (c) higher magnification image of apatite-like structure and (d) EDX analysis (spot at X) of the glass ceramic after immersion in SBF for 14 days

ACKNOWLEDGEMENTS

The authors would like to thank the Ministry of Higher Education (MOHE), Malaysia for the Fundamental Research Grant Scheme No. 9003-00483.

REFERENCES

Araújo, M., Miola, M., Baldi, G., Perez, J. & Verné, E. 2016. Bioactive glasses with low Ca/P ratio and enhanced bioactivity. *Materials* 226(9): 1-15.

Bellucci, D., Cannillo, V. & Sola, A. 2010. An overview of the effects of thermal processing on bioactive glasses. *Science of Sintering* 42(3): 307-320.

Bizari, D., Rabiee, M., Moztarzadeh, F., Tahriri, M., Alavi, S.H. & Masaeli, R. 2013. Synthesis, characterization and biological evaluation of sol-gel derived nanomaterial in the ternary system 64% SiO_2-31% CaO-5% P_2O_5 as a bioactive glass: *In vitro* study. *Ceramics - Silikaty* 57 (3): 201-209.

Brink, M., Turunen, T., Happonen, R.P. & Yli-Urpo, A. 1997. Compositional dependence of bioactivity of glasses in the system Na_2O-K_2O-MgO-CaO-B_2O_3-P_2O_5-SiO_2. *Journal of Biomedical Materials Research* 37(1): 114-121.

Chen, Q.Z., Li, Y., Jin, L.Y., Quinn, J.M.W. & Komesaroff, P.A. 2010. A new sol - gel process for producing Na_2O-containing bioactive glass ceramics. *Acta Biomaterialia* 6: 4143-4153.

Chen, Q.Z. & Boccaccini, A.R. 2006. Coupling mechanical competence and bioresorbability in bioglass ® -derived tissue engineering scaffolds. *Advanced Engineering Materials* 8(4): 285-289.

Chen, Q.Z., Thompson, I.D. & Boccaccini, A.R. 2006. 45S5 Bioglass-derived glass-ceramic scaffolds for bone tissue engineering. *Biomaterials* 27(11): 2414-2425.

Delben, J.R.J., Pereira, K., Oliveira, S.L., Alencar, L.D.S., Hernandes, A.C. & Delben, A.A.S.T. 2013. Bioactive glass prepared by sol-gel emulsion. *Journal of Non-Crystalline Solids* 361: 119-123.

Duée, C., Désanglois, F., Lebecq, I., Moreau, G., Leriche, A. & Follet-Houttemane, C. 2007. Mixture designs applied to glass bioactivity evaluation in the Si-Ca-Na system. *Journal of Non Crystalline Solids* 355(16-17): 943-950.

Esfehani, F., Baghshaei, S. & Ghader, A.A.B. 2013. The effects of CaO/P_2O_5 molar ratio changes on *in vitro* bioactivity of nanopowder glass via sol-gel in SiO_2-CaO-P_2O_5 system. *Basic and Applied Scientific Research* 3(1s): 375-382.

Guarino, V., Causa, F. & Ambrosio, L. 2007. Bioactive scaffolds for bone and ligament tissue. *Expert Review of Medical Devices* 4(3): 405-418.

Izadi, S., Hesaraki, S. & Ardakani, M.H. 2014. Evaluation nanostructure properties of bioactive glass scaffolds for bone tissue engineering. *Advanced Materials Research* 829: 289-293.

Izquierdo, B., Isabel, A. & Salinas, J. 1999. *In vitro* calcium phosphate layer formation on sol-gel glasses of the system CaO-SiO_2. *Biomedical Materials Research* 4636: 243-250.

Jones, J.R., Lin, S., Yue, S., Lee, P.D., Hanna, J.V. & Newport, R.J. 2010. Bioactive glass scaffolds for bone regeneration and their hierarchical characterisation. *Engineering in Medicine* 224: 1373-1387.

Jones, J.R. 2009. New trends in bioactive scaffolds: The importance of nanostructure. *Journal of the European Ceramic Society* 29: 1275-1281.

Jones, J.R., Ehrenfried, L.M. & Hench, L.L. 2006. Optimising bioactive glass scaffolds for bone tissue engineering. *Biomaterials* 27: 964-973.

Kamalian, R., Yazdanpanah, A., Moztarzadeh, F., Ravarian, R., Moztarzadeh, Z., Tahmasbi, M. & Mozafari, M. 2012. Synthesis and characterization of bioactive glass/forsterite nanocomposites for bone and dental implants. *Ceramics - Silikaty* 56(4): 331-340.

Karageorgiou, V. & Kaplan, D. 2005. Porosity of 3D biomaterial scaffolds and osteogenesis. *Biomaterials* 26: 5474-5491.

Liu, J. & Miao, X. 2004. Sol-gel derived bioglass as a coating material for porous alumina scaffolds. *Ceramics International* 30: 1781-1785.

Liu, X., Rahaman, M.N. & Fu, Q. 2013a. Bone regeneration in strong porous bioactive glass scaffolds with an oriented microstructure implanted in rat calvarial defects. *Acta Biomaterialia* 9(1): 4889-4898.

Liu, X., Rahaman, M.N., Hilmas, G.E. & Bala, B.S. 2013b. Mechanical properties of bioactive glass scaffolds fabricated by robotic deposition for structural bone repair. *Acta Biomaterialia* 9(6): 7025-7034.

Mami, M., Lucas-Girot, A., Oudadesse, H. & Dorbez-Sridi, R. 2008. Investigation of the surface reactivity of a sol-gel derived glass in the ternary system SiO_2–CaO–P_2O_5. *Applied Surface Science* 254: 7386-7393.

Mehdikhani, B. & Borhani, G.H. 2013. Crystallization behavior and microstructure of bio glass-ceramic system. *International Letters of Chemistry* 14: 58-68.

Mozafari, M., Moztarzadeh, F. & Tahriri, M. 2010. Investigation of the physico-chemical reactivity of a mesoporous bioactive SiO_2–CaO–P_2O_5 glass in simulated body fluid. *Non Crystalline Solids* 356(28): 1470-1478.

Mukundan, L.M., Nirmal, R., Vaikkath, D. & Nair, P.D. 2013. A new synthesis route to high surface area sol gel bioactive glass through alcohol washing. A preliminary study. *Biomatter* 3: 1-10.

Nandi, S.K., Kundu, B. & Datta, S. 2011. Development and applications of varieties of bioactive glass compositions in dental surgery, third generation tissue engineering, orthopaedic surgery and as drug delivery system. In *Biomaterials Applications for Nanomedicine,* edited by Pignatello, R. Croatia: Intech. Chapter 4. pp. 69-116.

Rezwan, K., Chen, Q.Z., Blaker, J.J. & Roberto, A. 2006. Biodegradable and bioactive porous polymer/inorganic composite scaffolds for bone tissue engineering. *Biomaterials* 27: 3413-3431.

Saboori, A., Rabiee, M., Moztarzadeh, F., Sheikhi, M., Tahriri, M. & Karimi, M. 2009. Synthesis, characterization and *in vitro* bioactivity of sol-gel-derived SiO_2-CaO-P_2O_5-MgO bioglass. *Materials Science and Engineering C* 29(1): 335-340.

Sabree, I., Gough, J.E. & Derby, B. 2015. Mechanical properties of porous ceramic scaffolds: Influence of internal dimensions. *Ceramics International* 41: 8425-8432.

Saravanapavan, P. & Hench, L.L. 2003. Mesoporous calcium silicate glasses. I. Synthesis. *Journal of Non-Crystalline Solids* 318: 1-13.

Saravanapavan, P., Jones, J.R., Pryce, R.S. & Hench, L.L. 2003. Bioactivity of gel–glass powders in the CaO-SiO_2 system: A comparison with ternary (CaO-P_2O_5-SiO_2) and quaternary glasses (SiO_2-CaO-P_2O_5-Na2O). *Journal of Biomedical Materials Research Part A* 66(1): 110-119.

Shu, C., Wenjuan, Z., Xu, G., Wei, Z., Wei, J. & Dongmei, W. 2010. Dissolution behavior and bioactivity study of glass ceramic scaffolds in the system of CaO–P_2O_5–Na_2O–ZnO prepared by sol-gel technique. *Materials Science and Engineering C* 30: 105-111.

Siqueira, R.L., Peitl, O. & Zanotto, E.D. 2011. Gel-derived SiO_2–CaO–Na_2O–P_2O_5 bioactive powders: Synthesis and *in vitro* bioactivity. *Materials Science and Engineering C* 31: 983-991.

Stábile, F.M., Martinez Stagnaro, S.Y., Ortiga, J. & Volzone, C. 2015. Production of porous scaffolds from bioglass 45S5-derived glasses. *Procedia Materials Science* 9: 558-562.

Wachi, S. & Jones, A.G. 1992. Dynamic modelling of particle size distribution and degree of agglomeration during precipitation. *Chemical Engineering Science* 47(12): 3145-3148.

Wu, Z.Y., Hill, R.G. & Jones, J.R. 2011. Optimizing the processing of porous melt-derived bioactive glass scaffolds. *Bioceramics Development and Applications* 1: 2-5.

Syed Nuzul Fadzli Syed Adam* & Roslinda Shamsudin
School of Applied Physics
Faculty of Science and Technology
Universiti Kebangsaan Malaysia
43600 UKM Bangi, Selangor Darul Ehsan
Malaysia

Siti Rohani Zainuddin, Banjuraizah Johar & Firuz Zainuddin
School of Materials Engineering
Universiti Malaysia Perlis
02600 Arau, Perlis Indera Kayangan
Malaysia

*Corresponding author; email: syed.nuzul@unimap.edu.my

Received: 15 September 2017
Accepted: 20 November 2017